2014-01-1231
Published 04/01/2014
doi:10.4271/2014-01-1231
saefuel.saejournals.org

Intermediate Alcohol-Gasoline Blends, Fuels for Enabling Increased Engine Efficiency and Powertrain Possibilities

Derek Splitter and James Szybist
Oak Ridge National Lab.

ABSTRACT

The present study experimentally investigates spark-ignited combustion with 87 AKI E0 gasoline in its neat form and in mid-level alcohol-gasoline blends with 24% vol./vol. iso-butanol-gasoline (IB24) and 30% vol./vol. ethanol-gasoline (E30). A single-cylinder research engine is used with a low and high compression ratio of 9.2:1 and 11.85:1 respectively. The engine is equipped with hydraulically actuated valves, laboratory intake air, and is capable of external exhaust gas recirculation (EGR). All fuels are operated to full-load conditions with λ=1, using both 0% and 15% external cooled EGR. The results demonstrate that higher octane number bio-fuels better utilize higher compression ratios with high stoichiometric torque capability. Specifically, the unique properties of ethanol enabled a doubling of the stoichiometric torque capability with the 11.85:1 compression ratio using E30 as compared to 87 AKI, up to 20 bar $IMEP_g$ at λ=1 (with 15% EGR, 18.5 bar with 0% EGR). EGR was shown to provide thermodynamic advantages with all fuels. The results demonstrate that E30 may further the downsizing and downspeeding of engines by achieving increased low speed torque, even with high compression ratios. The results suggest that at mid-level alcohol-gasoline blends, engine and vehicle optimization can offset the reduced fuel energy content of alcohol-gasoline blends, and likely reduce vehicle fuel consumption and tailpipe CO_2 emissions.

CITATION: Splitter, D. and Szybist, J., "Intermediate Alcohol-Gasoline Blends, Fuels for Enabling Increased Engine Efficiency and Powertrain Possibilities," *SAE Int. J. Fuels Lubr.* 7(1):2014, doi:10.4271/2014-01-1231.

INTRODUCTION

The Energy Independence and Security Act of 2007 [1], requires that by year 2022, 36 billion gallons per year of bio-derived fuels be consumed in transportation. This uptake in bio-derived fuels is more than a seven-fold increase from the 4.7 billion gallons consumed per year when the law was enacted. The rules for complying with this mandate are specified by the U.S. Environmental Protection Agency (EPA) in the Renewable Fuel Standard II (RFS II) [2].When the total transportation energy consumption is analyzed, it is apparent that this legislation increases the usage of bio-fuels. In 2012 the United States consumed 27.97 quadrillion BTU of energy for transportation, and is projected to consume 29.24 quadrillion BTU in 2022 [3]. Assuming a gasoline equivalent energy of 42.8 MJ/kg, and density of 740 kg/m^3, the RFS II standard will require an increase in the volumetric percentage of transportation energy from biofuels to approximately 14% in 2022 from the approximately 2% in 2007. To date, the RFS II progress has seen more than a doubling of biofuel usage, with the annual recorded share of transportation energy from non-petroleum sources totaling 4.3% in 2012. Although 2012 was the year with the largest biofuel energy share on record [3], there is still an additional threefold increase in biofuel energy share required to comply with the RFS II mandate.

Concurrent with RFS II, legislation by the National Highway and Transportation Safety Administration passed in 2011 requires corporate average fuel economy (CAFE) standards to achieve 54.5 US miles per gallon by 2025 [4], an effective two fold increase compared with present CAFE standards. Ideally, the RFS II and CAFE mandates could be met simultaneously through proper exploration and implementation of high-efficiency bio-fuel engines.

In the United States, the stoichiometrically operated spark ignition (SI) engine has maintained over a 99% market share in the light-duty (LD) vehicle sector (passenger cars and pickup trucks) since 1985 [5] and over a 94% share since the EPA began record keeping in 1975. This LD sector engine dominance is due primarily to the facts that the SI engine has: low production cost, low fuel cost, rugged operation, high torque/power density, low sooting tendency, and can employ known mature catalyst technologies to reduce regulated emissions (oxides of nitrogen (NO_x), hydrocarbon (HC), and carbon monoxide (CO)). The market sector dominance with the SI engine in combination of legislated CAFE and RFS II standards suggests that increases to SI engine efficiency with bio-fuels might offer a very plausible path toward simultaneous CAFE and RFS II compliance.

Although the SI engine has many beneficial attributes, its efficiency is fundamentally hindered by the throttling of air, and its compression ratio is limited by combustion knock. These two factors result in lower thermal efficiency[1] of SI engines relative to compression-ignited engines (i.e., diesel engines) or lean-burn SI engines. Historically, engine improvements have focused primarily on increasing safety and convenience, yielding increases in performance and vehicle weight, while complying with legislated fuel economy mandates, which have been near-constant since 1985 [5]. The progress in engine performance over the years can clearly be observed when viewed relative to a 1975 baseline (the first year of EPA records): in today's vehicles the industry average power per unit displacement has more than doubled, while vehicle zero to 60 miles per hour acceleration time has halved [5]. This evolutionary increase in performance has resulted in a 50% reduction in the average light-duty engine displacement compared with a 1975 era engine. Although these trends show there has been significant progress in engine performance, to comply with future CAFE requirements, engine and vehicle efficiency must also be addressed and improved.

An evolutionary strategy for achieving CAFE compliance while retaining performance is downsizing and turbocharging with direct injection. These two technologies offer increased engine power/torque density, with similar performance when downsizing and downspeeding engines, a proven efficiency improving strategy [6]. However, the opportunity for downsizing and downspeeding becomes limited by combustion knock from current market available fuels, thereby limiting thermodynamic efficiency.

Unlike distillate fuels, alcohol fuels exhibit some key properties that make them particularly attractive fuels for future engines. Most notably, alcohol fuels tend to have a high octane number and lower carbon intensity.[2] These combinations of properties grant alcohol-based fuels a twofold reduction potential in tailpipe carbon dioxide (CO_2) through molecular advantage and the ability to tolerate higher engine compression ratios. Additionally, alcohol fuels exhibit two other properties that can be favorable for increasing engine efficiency:

First, alcohol fuels exhibit a high latent heat of vaporization (HoV), which, when used in conjunction with direct injection (DI) fueling, can increase the incoming charge density caused by a reduction in charge temperature. When exploited properly, the high HoV improves engine breathing as highlighted Stein et al. [7], and mitigates combustion knock tendency. The effect of HoV has proved to be strong, even in a sparingly used dual-fuel arrangement, where the charge cooling of a small amount of direct injected ethanol prevented knock and extended the torque capability [8], with both benefits enabling higher efficiency engines.

Second, the amount of thermodynamic work that can be extracted from alcohols on a 2nd law basis is higher than is suggested by its lower heating value (LHV) alone (i.e., exergy/LHV). This is attributed to a high yield of molar products for alcohols on both a stoichiometric and energy basis relative to petroleum distillates, increasing expansion pressure [9, 10]. Ford and AVL have shown that ethanol enables efficiency improvements, with several notable works summarized in Stein et al. [11]. Vehicle-specific effects were researched by Jung et al. [12] at light load conditions and also in an additional study by Jung et al. [13] with drive cycle and engine efficiency estimates. The latter study points out that a light-duty pickup truck engine with intermediate ethanol-gasoline blends could be optimized such that the thermal efficiency increase with ethanol-gasoline blends of 20% ethanol vol./vol. are sufficiently high to at least offset the volumetric energy density penalty of alcohol fuels, and achieve even greater tailpipe CO_2 reductions.

These engine experiments and vehicle simulation results demonstrate that reductions in CO_2 emissions without a decrease in miles per gallon (MPG) could be possible with intermediate ethanol-gasoline blends. A major reason for this prediction is the ability of ethanol addition to reduce combustion knock and enable an increased compression ratio. Interestingly, work by Szybist and West [14] demonstrates that blending ethanol, even with very low-octane gasoline blendstocks, offers significant anti-knock resistance and that a high-octane fuel can be produced through blending intermediate levels of ethanol with straight-run gasoline. This is because of the highly nonlinear response of octane number blending with ethanol on a volumetric basis, as previously explained in detail by Anderson et al. [15, 16], and more recently by Foong et al.[17]. These cited studies show that intermediate-level ethanol blends might be promising for the next generation of SI engine fuels. The noted inherent benefits provide the potential to increase the power output and efficiency of the engine through fuel based knock mitigation coupled to engine optimization. However, as pointed out in the 2013 SAE International High Octane Fuel Symposium [18], multiple levels of cooperation from the fuel industry, legislation and regulatory bodies, distribution systems, and point of sale vendors is required if fuel octane is to be increased.

The use of external cooled exhaust gas recirculation (EGR) could be a more direct approach to increasing SI engine efficiency. External EGR is a proven method to reduce the knocking tendency for a given fuel. External-cooled EGR has been employed for years in diesel engines, with recent interest gaining in SI engines. The constituents of EGR in SI engines differ from those in their diesel counterparts. Specifically, $\lambda=1$ SI EGR is oxygen deficient, meaning that SI EGR offers the potential to increase charge mass without changing the oxygen content. The lack of oxygen in SI EGR is important when considering both catalyst and throttling requirements of SI engines (i.e., $\lambda=1$). In addition to reducing throttling losses, the introduction of EGR into SI engines improves the

1 Defined as the efficiency of converting fuel chemical energy to mechanical output work

2 Defined as the number of moles of carbon per unit of energy (LHV)

thermodynamic properties of the working fluid (i.e., the ratio of specific heats (γ)), reducing in-cylinder temperatures and improving knock resistance.

Many of these thermodynamic advantages have been documented by others. For example, Alger et al. [19] showed that external-cooled EGR effectively decreased the knocking propensity of distillate fuel which functionally increased the fuel octane number. However, EGR also slowed the flame kernel growth because of slowed reaction rates. These EGR combustion process and anti-knock findings were furthered by the inclusion of intermediate alcohol-gasoline blends in Splitter and Szybist [20], which showed that 15 % external cooled EGR effectively negated the increased burning velocities intrinsic with alcohol fuels [21, 22]. Therefore, regardless of fuel type, higher EGR levels in SI engines might require the incorporation of different higher turbulence combustion chamber flows to increase EGR tolerance, as shown by Wheeler at al. [23], or through high-energy long spark systems as shown by Alger et al. [24]. These previous studies suggest there are technical challenges that need to be addressed if EGR is to be used.

The relations between knock mitigation and cycle difference with external cooled EGR raise several questions:

- What, if any, role does EGR have on engine efficiency in mid-level alcohol blends?
- What are the combustion specific differences between intermediate alcohol-gasoline blends and neat gasoline?
- What, if any, potential performance and fuel economy incentives do mid-level alcohol blends offer both with and without external cooled EGR?
- Can intermediate alcohol-gasoline fuels enable new powertrain possibilities?

The present study explores what engine efficiency and stoichiometric torque capability gains can be enabled through the use of mid-level ethanol and iso-butanol gasoline blends as compared to conventional gasoline. The engine efficiency, load-speed range, and downsizing + downspeeding potential of each strategy and fuel is investigated relative to one another using a higher than stock 11.85 r_c piston and compared to 87AKI gasoline with the production 9.2 r_c piston.

EXPERIMENTAL DETAILS

This study explores SI engine operation at 5 engines speeds (1200, 1600, 2000, 2500, and 3000 r/min) and two different EGR rates (0% and 15%), each with three different fuels (87AKI E0 “regular” gasoline, 30% by vol. ethanol-gasoline, and 24% by vol. iso-butanol-gasoline). A highly modified 2.0 L GM Ecotec SI engine with stock side-mounted direct fuel injector is used. Three cylinders of the production engine are disabled to allow single-cylinder operation with an installed custom-domed piston, which increases the compression ratio to 11.85:1 (stock 9.2:1).

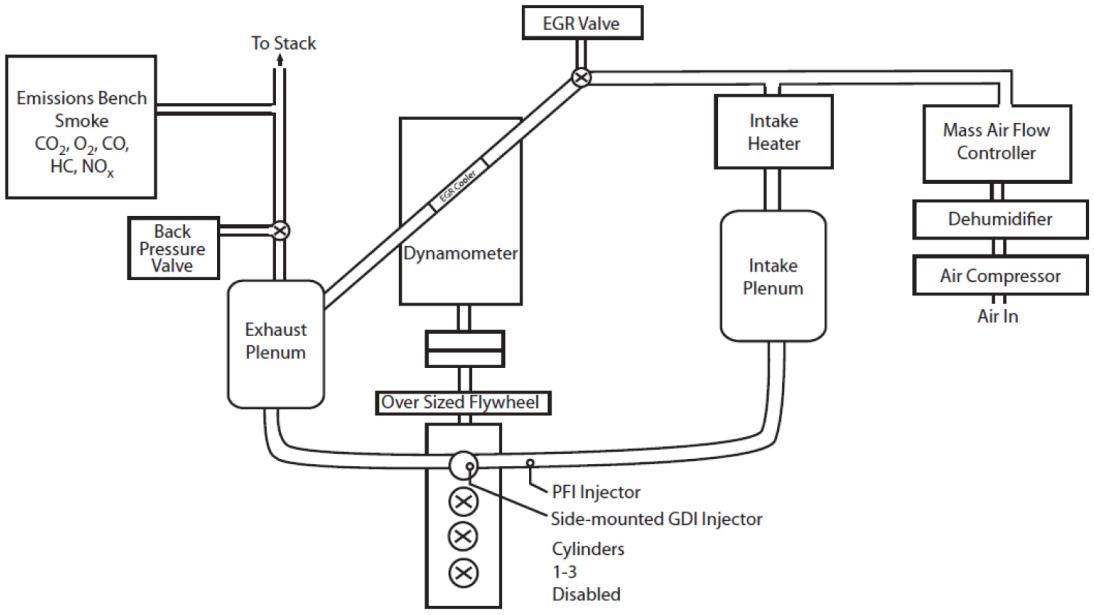

Figure 1. Schematic of the experimental configuration.

The SI engine is operated with a laboratory air handling system. Pressurized and dried facility air that has less than 5% relative humidity is metered to the engine using a mass air flow controller. The present study omits humidity effects, where added humidity may have an effect of reducing knock. The engine is equipped with separate electro-mechanical valves for backpressure and external EGR, enabling the capability for independent control of intake manifold pressure, exhaust manifold pressure, and EGR. Cooled EGR mixes with fresh air upstream of an air heater, followed by the intake plenum and then the intake manifold. The arrangement results in the intake manifold temperature being controlled to constant a set temperature (52°C) regardless of EGR rate. EGR is measured using an EGR 5230 system from ECM, an instrument that uses pressure-compensated wideband oxygen sensors in both the intake and exhaust to non-intrusively measure EGR. When EGR is used, a constant rate of 15±1% is supplied. A schematic of the laboratory is provided in Figure 1.

The engine is equipped with a hydraulic valve actuation (HVA) system to enable fully variable valve actuation. To accommodate the small research module HVA system from Sturman Industries, the cylinder head has been machined, disabling the functionality of the production cam and fuel pump systems. Details of the VVA system have been published previously [9, 25,26]. The engine geometry is listed in Table 1.

Table 1. Engine geometry

Bore x Stroke	86mm x 86mm
Connecting rod length	145.5mm
Compression ratios	9.2 (stock), 11.85:1 (modified)
Fuel injection system	Direct injection, side-mounted

Crank-angle (CA) resolved data are recorded at 1800 samples per revolution (0.2°CA resolution) for 300 consecutive cycles. Cylinder pressure is measured using a Kistler piezo-electric 6125B pressure transducer coupled to a Kistler 5010 charge amplifier. Additionally, the DI command signal and intake and exhaust valve lift from each of the four HVA valves is recorded on a crank-angle resolved basis. All indicated results presented in this study are for a 300 cycle average.

Engine emissions are measured using a standard emissions bench with instruments manufactured by California Analytical Instruments. NO_x is measured using a heated chemiluminescence analyzer, CO and CO_2 are measured using infrared analyzers, oxygen (O_2) is measured using a paramagnetic analyzer, and HC is measured with a heated flame ionization detector. Smoke measurements are performed using an AVL 415s filter smoke number (FSN) instrument. To measure the fuel flow rate (and thus efficiency), the air-to-fuel ratio (AFR) is measured directly from a Coriolis-effect fuel flow meter and a laminar air flow element. The corresponding fuel flow is then cross referenced to independently calculate air-to-fuel ratios from the engine exhaust using both the emissions bench and automotive wideband oxygen sensor approaches.

The conditions for all fuels, engine speeds, loads, and EGR combinations are listed in Table 2.

Table 2. Constant operating conditions

Exhaust valve open at 0.8 mm lift (°CA $ATDC_f$)	170
Exhaust valve close at 0.8 mm lift (°CA $ATDC_f$)	350
Max exhaust valve lift (mm)	9
Intake valve open at 0.8 mm lift (°CA $ATDC_f$)	-355
Intake valve close at 0.8 mm lift (°CA $ATDC_f$)	-170
Max intake valve lift (mm)	9
Start of DI command (°CA $ATDC_f$)	-280
Intake manifold gas temperature (°C)	52
Engine coolant (°C)	90
Oil (°C)	90
Exhaust λ (-)	1
DI rail pressure (bar)	100

Five engine speeds of 1200, 1600, 2000, 2500, and 3000 r/min are tested with gross load increments ($IMEP_g$ indicating mean effective pressure gross) of 50±5 kPa. The constraints and load range for E30 without EGR can be seen in Figure 2, which illustrates the tested operational map up to the constraints for E30 with 0% EGR. The identical procedure and setup is conducted for each fuel type and both EGR rates.

All fuels and EGR rates are tested at maximum brake torque (MBT) timing until combustion knock is encountered. Once knock limited, combustion is phased through spark timing to maintain a constant level of knock through visual inspection of the indicated pressure trace and by maintaining constant AVL combustion noise, which were empirically found to trend together. The tested load range is from 2 bar $IMEP_g$ to full load, which is defined as the maximum load without enrichment (λ=1) with limits on CA50 (crank angle at 50% mass fraction burned) combustion phasing of 25°CA $ATDC_f$, peak cylinder pressure of 10,000 kPa, and exhaust gas temperature (EGT) of 800°C. (Note: CA50 combustion phasing later than 25°CA $ATDC_f$ is not ideal for high efficiency, which is the focus of the present study. Additionally, 800°C EGT limit is imposed

because unlike the production engine, the Sturman valvetrain does not use sodium-filled values which can withstand higher exhaust gas temperatures. The maximum cylinder pressure limit is set because the stock engine is rated to 10,000 kPa, although this constraint is not reached by any of the present fuel or experimental condition combinations). Figure 2 displays the constraint limits reached with 0% EGR E30 operation.

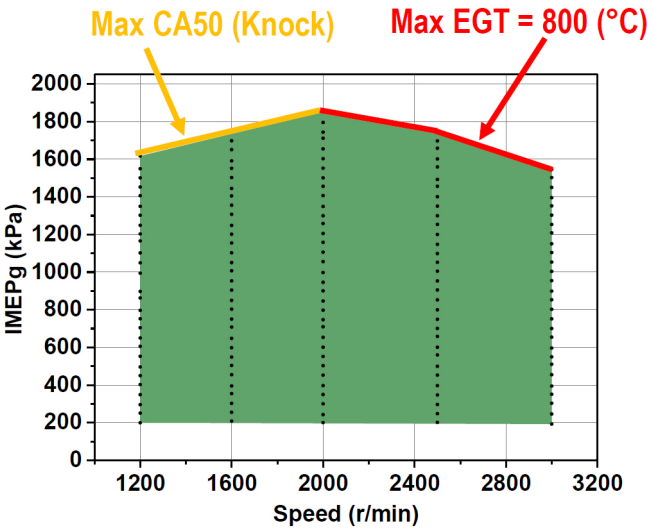

Figure 2. Representative engine load-speed range tested with knock and EGT constraints indicated.

The only exception to the constraints is at the lightest loads with EGR ($IMEP_g \leq 250$ kPa), where combustion is unstable at MBT CA50 phasing, where later than MBT CA50 were found to improve stability. The constraint used to bound the amount of CA50 retard for acceptable operation at these lightest loads is $CA50 \leq 15°CA\ ATDC_f$. Using these limits, operation with each fuel was compared.

The production spark plug heat range and gap is used for all tests. However, the spark energy is generated with an aftermarket MSD DIS6-2 Plus multi-strike ignition system to increase the combustion stability at high EGR levels. The MSD system is capable of up to three consecutive spark discharges per cycle, but the number of discharges is speed dependent, with only one or two discharges at higher engine speeds. The spark coil signal from the MSD system, heat release rate (HRR), and cylinder pressure are indicated in Figure 3, along with the unique valve events provided by the Sturman HVA system. The near square valve lift profile generated by the Sturman HVA system differs from conventional valve lift and duration dynamics, resulting in increased flow area with different engine breathing and charge motion characteristics. The specific differences between the HVA valvetrain and a cam-based valvetrain are discussed in a previous publication [26].

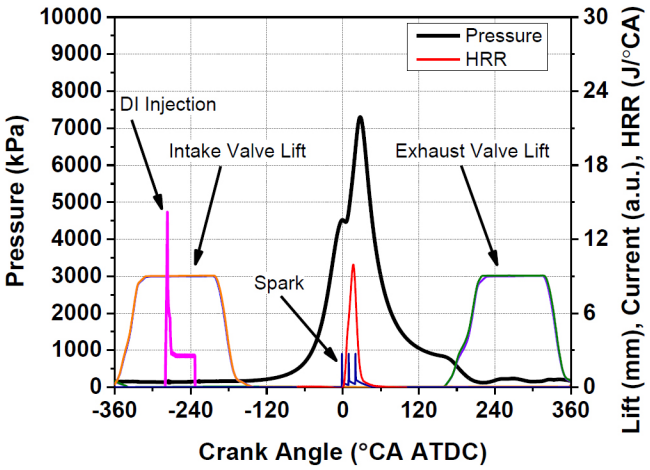

Figure 3. Representative high-load fired case showing indicated cylinder pressure, apparent heat release rate (HRR) with corresponding valve, spark, and injection event schedule.

When operating with higher than atmospheric pressures, a constant overall turbocharger efficiency of 25% with no intake or exhaust pressure restrictions is assumed (i.e., no muffler pipe, catalysis, or air cleaner pressure losses assumed). This assumption is considered valid and conservative because the production turbocharger for this SI engine is capable of over 55% combined overall efficiency. The combined turbocharger efficiency is calculated based on the air standard model as explained in Heywood [27] (Equation1), using intake and exhaust surge tank pressures and temperatures measured in the ports and assuming 100% turbine shaft mechanical efficiency.

$$\eta_{combined} = \frac{\left(\frac{\gamma_{comp}}{\gamma_{comp}-1}\right)}{\left(\frac{\gamma_{turb}}{\gamma_{turb}-1}\right)}\left(\frac{T_{comp,in}}{T_{turb,in}}\right)\frac{\left[\left(\frac{P_{comp,in}}{P_{comp,out}}\right)^{\left(\frac{\gamma_{comp}-1}{\gamma_{comp}}\right)}-1\right]}{\left(1+\frac{1}{AFR}\right)\left[1-\left(\frac{P_{turb,out}}{P_{turb,in}}\right)^{\left(\frac{\gamma_{turb}-1}{\gamma_{turb}}\right)}\right]} \quad (1)$$

When operating with external EGR, the electromechanical valves for backpressure and EGR were modulated as needed to maintain 15% EGR and 25% combined turbocharger efficiency.

Fuels and Fuel Properties

Three fuels are tested: two fuels are alcohol-gasoline blends, and the third is an unblended gasoline. The two alcohol blended fuels were splash blended on site with either 24% neat iso-butanol or 30% neat-ethanol, with alcohol and gasoline volume fractions being measured in un-blended fractions and then combined. All fuels were based on commercially obtained 87 AKI E0 “regular” pump fuel sourced directly from a distribution terminal. It should be noted that splash blending

these alcohols with finished market E0 gasoline is not likely at an industrial scale if the tested blend ratios were to be market sold. More likely, a blendstock for oxygenate blends (BOB) fuel would be used, which tend to have lower octane numbers. Although using a BOB would decrease the research octane number (RON) of a blended fuel below those tested in the present study, others studies, [7, 14] have shown that the RON difference of a blended fuel based on a BOB vs. a finished E0 is much smaller than the difference in RON between the unblended BOB and finished E0 fuels.

Table 3. Fuel properties.

	87 AKI	IB24	E30
Oxygenates ASTM D5599 (%v)	<0.1 any	23.64 iso-butanol	30.65 ethanol
HoV (kJ/kg)[3]	352[31, 32]	443 [31, 31, 33]	529 [31, 31, 33]
HoV with gasoline energy eq.[4] (kJ/kg)	352 [31, 32]	470 [31, 32, 33]	599 [31, 32, 33]
Reid vapor pressure, ASTM D5191 (psi)	13.13	12.29	13.28
10% distillation point, ASTM D86 (°F)	97	115	111
30% distillation point, ASTM D86 (°F)	144	175	150
50% distillation point, ASTM D86 (°F)	205	208	165
70% distillation point, ASTM D86 (°F)	253	222	170
90% distillation point, ASTM D86 (°F)	316	307	299
RON, ASTM D2699(-)	90.2	96.6	100.3
MON, ASTM D2700(-)	83.9	86.8	88.8
Octane Sensitivity (-)	6.3	9.8	11.5
LHV, ASTM D240 (MJ/kg)	43.454	40.846	38.105
λ=1 AFR (-)	14.70	14.13	12.85
C, ASTM D5391 wt. (%)	86.49	80.63	74.4
H, ASTM D5391 wt. (%)	14.06	13.89	13.73
O, ASTM D5599 wt (%)	<0.1	3.71	11.34
Specific gravity, ASTMD4052(-)	0.729	0.743	0.745
Volumetric energy density (MJ/gal)	119.5	114.5	107.1

3 Calculated through a linear combination of neat alcohol and gasoline HoV.
4 Calculated on a gasoline equivalent energy basis, i.e., fueling required for matched load.

The blending ratios used are based on the following:

- 24% iso-butanol was selected as it has near identical oxygen content as E15, which the EPA has approved for use in 2001 and newer light duty vehicles [28,29].
- The 30% ethanol blend was selected because, as the EPA recently stated, [30] there is no foreseeable issue with higher ethanol-gasoline blends; citing blends as high as E30 would likely be permissible.

These alcohol-gasoline fuel blends are of interest as the neat alcohols used exhibit nearly identical motor octane number (MON) values and similar RON values [31]. However, the energy density of iso-butanol is higher than that of ethanol on both a volume and mass basis, thus making its energy density closer to a gasoline. Additionally, the lower water solubility of iso-butanol as compared to ethanol offers advantages in certain markets such as marine environments where humidity and water contact are more prone. Interestingly, research by Stein et al. [11] has demonstrated that the Reid vapor pressure of intermediate ethanol blends are typically lower than E10 blends for the same blendstock, making such fuels attractive to regulatory bodies, as has been indicated in the recent EPA Tier III notification of proposed rulemaking [30].

In the present study, the alcohols are from non-denatured reagent grade purity and obtained directly from suppliers. Sigma-Aldrich supplied the iso-butanol at a purity of >99%, and Decon Labs supplied the non-denatured ethanol. The three fuels were sent for independent analysis at an ASTM International certified laboratory. The key fuel properties from the analysis are presented in Table 3.

Results

The results section is divided into subsections. The first provides an overview of the fuel-specific and compression ratio differences on the operable speed-load range and combustion process of the engine without EGR. The second provides estimates of brake thermal efficiency differences between the stock engine with 87AKI gasoline 0% EGR and the higher compression ratio piston E30 with 0 or 15% external EGR. The third subsection discusses downsizing and downspeeding considerations.

Fuel and Compression Ratio Specific Effects

All fuels are operated to the maximum load condition defined by the aforementioned combustion knock and EGT constraints in the experimental details section. Figure 4 presents the tested load range of all three fuels with 0% and 15% EGR (bottom and top sub-plots respectively), with the 11.85 r_c piston and 87AKI with the 9.2 r_c piston.

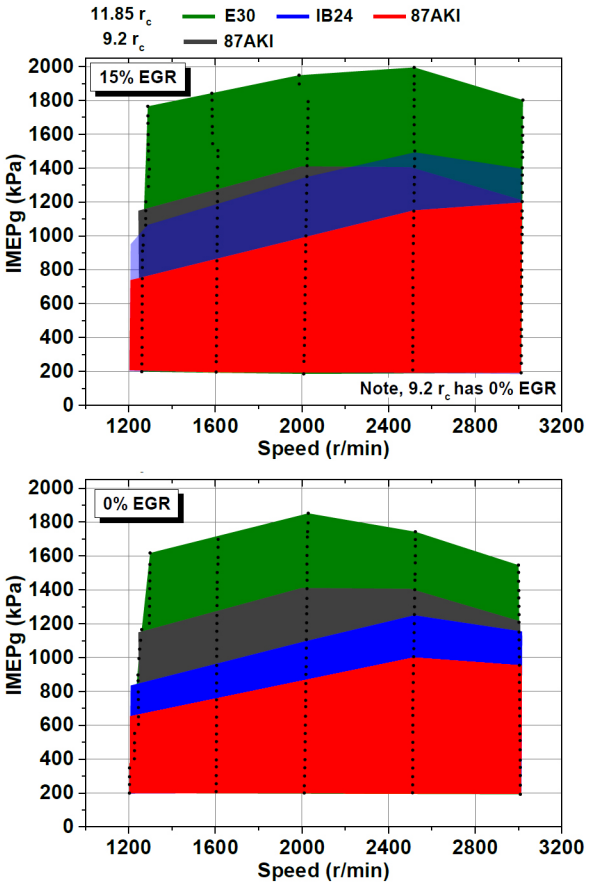

Figure 4. Load-speed range for all tested fuels, note small black dots depict measured data point.

As expected, the results in Figure 4 show that higher octane number fuels offer higher $IMEP_g$ at a given speed because of the improved resistance to knock. Although Figure 4 demonstrates that the load limit increases with octane number it does not provide detail into the onset of and behavior within the knock limited spark advance (KLSA) regime. The following sub-sections use a detailed combustion analysis to investigate fuel and compression ratio specific effects in greater detail.

Measured Combustion Process Differences

KLSA Phasing Effects

Figure 5 displays the CA50 combustion phasing requirements for all tested fuels and r_c at 2000 r/min.

The results exhibit two key findings. First, at a given r_c, the onset of knock is in agreement with the rated octane number. For example, with the 11.85 r_c, the load at which KLSA was required linearly increased with octane number (knock limit load of 87AKI<IB24<E30, respective RON 90.2, 96.6, 100.3). However, once knock limited, the effectiveness of CA50 retard is fuel specific. Specifically, as a function of knock limited load, phasing retard is more effective at mitigating knock with E30 than 87AKI. Research by Stein et al. [7] demonstrates similar trends, where a similar octane number distillate fuel will be more knock prone within KLSA than an ethanol-gasoline blend. That research attributes the increased knock tolerance of ethanol-gasoline blends to a combination of enthalpy of vaporization and chemical differences.

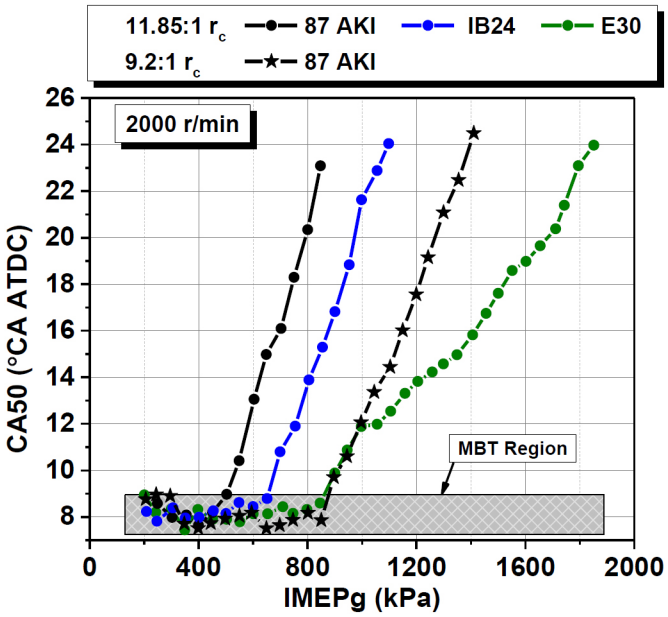

Figure 5. Combusiton CA50 phasing vs. load at 2000 r/min 0% EGR

The second observation from Figure 5, is that the load for the onset of knock between 87AKI 9.2 r_c and 11.85 r_c E30 is identical. Jung et al. [13] demonstrates that a 10 percent volume increase in ethanol with ethanol-gasoline blends enabled a 2 point increase in compression ratio with similar knock limited phasing. Their results were validated against E10 gasoline with E20 or E30 blends. That work demonstrates that in the knock limited regime ethanol content can affect the onset of and behavior within the knock limited operation. The present study further confirmed the findings of Jung's observations, in that a 2.65 point increase in compression yielded a similar load in the onset of knock as a 30 percentage difference in fuel ethanol volume percentage.

These two findings illustrate that the onset of knock behaves most similar to the fuel octane number and engine compression ratio, but that factors beyond octane number affect the behavior within the knock limited regime. Figure 5 demonstrates this difference at one speed, 2000 r/min.

To expand the comparison to more than one engine speed, the effects of speed on KLSA behavior are explored by analyzing the KLSA CA50 as a function of $IMEP_g$ in knock limited regime. The term "$IMEP_g$ in knock limited regime" is defined as the load after entering the knock limited regime, thus a value of 0 $IMEP_g$ denotes the knock limit of the respective fuel and compression ratio. Figure 6 illustrates the $IMEP_g$ in knock limited regime for all tested fuels with 0% EGR at 1200 and 3000 r/min operation, the speed extremes of the present study. Note that data with 87AKI is plotted with both tested compression ratios.

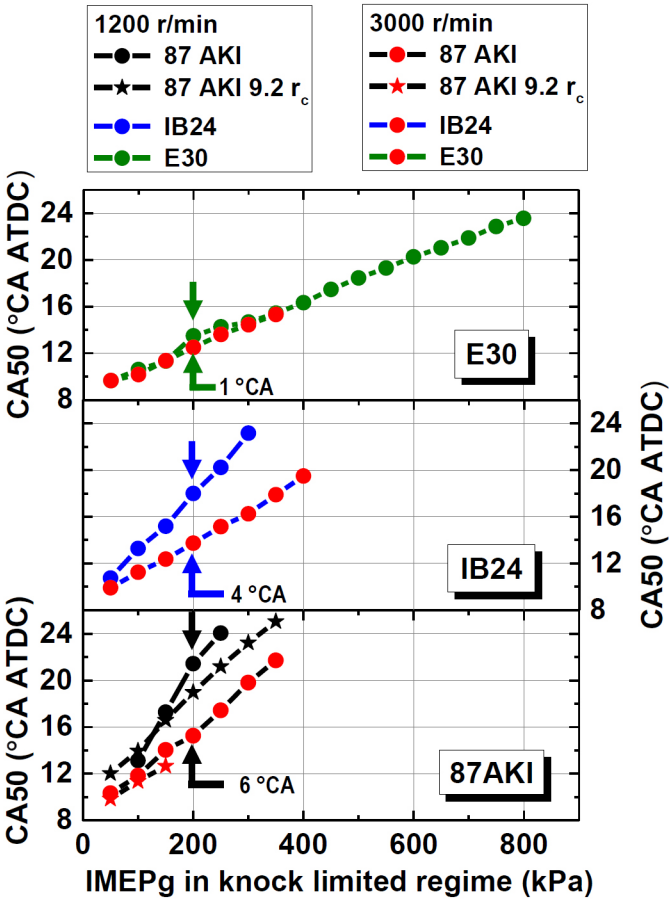

Figure 6. CA50 phasing requirement within the knock limited regime for all tested fuels at 1200 and 3000 r/min operation with 0% EGR.

The results illustrate that the CA50 phasing within the knock limited regime is a function of load, speed, and fuel type. For example, at 200 kPa IMEP$_g$ in the knock limited regime, the CA50 phasing spread between 3000 and 1200 r/min with 87AKI is 6°CA, IB24 is 4°CA, and E30 is 1°CA. Interestingly, this behavior appears to be independent of compression ratio as 87AKI displays similar CA50 phasing requirements as a function of IMEP$_g$ in the knock limited regime at both tested compression ratios. These results suggest that fuel properties are dominating the CA50 phasing requirements within the knock limited regime.

To better assess the phasing requirements across the entire tested engine speed range, the average CA50 as a function of IMEP$_g$ in the knock limited regime was calculated. The results of the speed averaging are plotted in Figure 7. Note that Figure 6 previously indicated that the maximum IMEP$_g$ in the knock limited regime was speed dependent (i.e., the 25°ATDC CA50 or 800°C EGT constraint are reached at different speeds and with different fuels). Therefore, Figure 7 uses different data markers types to illustrate the number of engine speeds incorporated into the average CA50 as a function of IMEP$_g$ in the knock limited regime. When all 5 speeds are averaged, a solid marker is used. When fewer than all speeds are averaged, an open marker is used. Also, a linearity line of the all averaged speed conditions is added for reference.

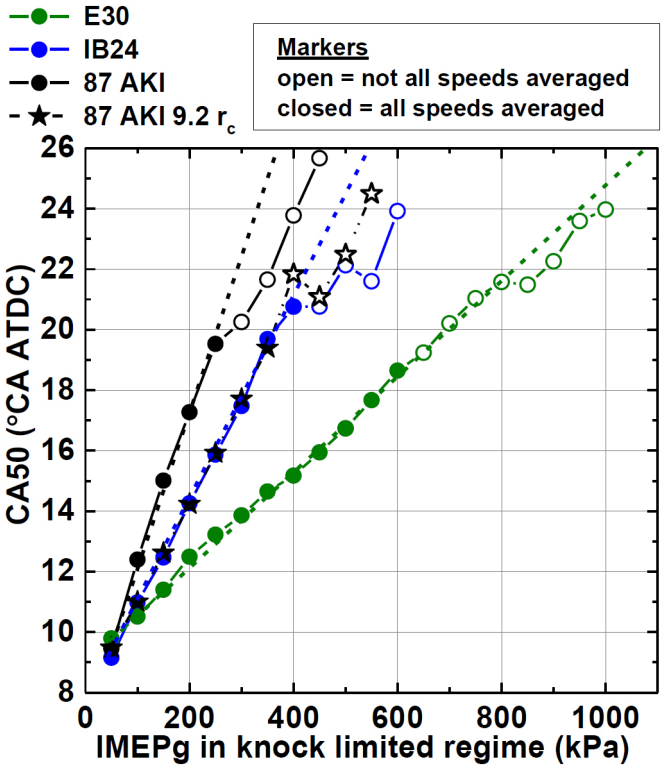

Figure 7. Average of all speeds with KLSA CA50 phasing, solid markers denote all speeds could be averageed, open markers denote less than all speeds could be averaged.

The results presented in Figure 7 are similar to the knock limit of the fuels (Figure 5) and the octane number sensitivity of the fuels (Table 3), which are ordered as 87AKI < IB24 < E30. However, Figure 7 shows that E30 is the least speed sensitive; because the open data markers remain on or near the all speeds averaged linear line (E30 open markers follow the all speeds dashed linearity line). Conversely, the open marker 87AKI data fall off the dashed linearity line at higher knock limited IMEP$_g$, illustrating that at faster engine speeds less phasing retard is required with 87AKI.

The octane number sensitivity (S) of a fuel is defined as the mathematical difference between RON and MON. As pointed out by Leppard [34], S is a measure of the extent to which the fuel differs from alkane fuels. This is because the octane number scale is based on n-heptane and iso-octane, alkanes,

which by definition have S=0. Likewise, the S of other normal and iso-alkanes follow the behavior of n-heptane and iso-octane, and exhibit very low S values. More recently, Mittal et al. [35] used computational simulations to show this effect with bio-fuels, which included a 96 RON ethanol-alkane blend. These two works support the present findings in that higher fuel sensitivity (S) has a more linear and predictable phasing requirement in the knock limited regime.

Notably, Figure 5 shows identical onset of knock between 87AKI 9.2 r_c and E30 11.85 r_c, but Figures 6 and 7 illustrate that within the knock limited regime, the CA50 phasing requirement 87AKI with the reduced 9.2 r_c is also reduced, and is very similar to IB24 at 11.85 r_c. These results indicate that the knock limited regime is somewhat less phasing dependent with the lower compression ratio, thereby increasing the authority that CA50 phasing has on knock mitigation with the lower compression ratio piston. A potential reason for this may be in combustion duration differences between the two pistons, discussed in the following section.

Combustion Duration Effects

It is well known that shorter combustion duration reduces the time-temperature history of the end gas, which reduces knocking tendency. Figure 8 illustrates the 5-50% mass fraction burned (MFB) of the different fuels and compression ratios.

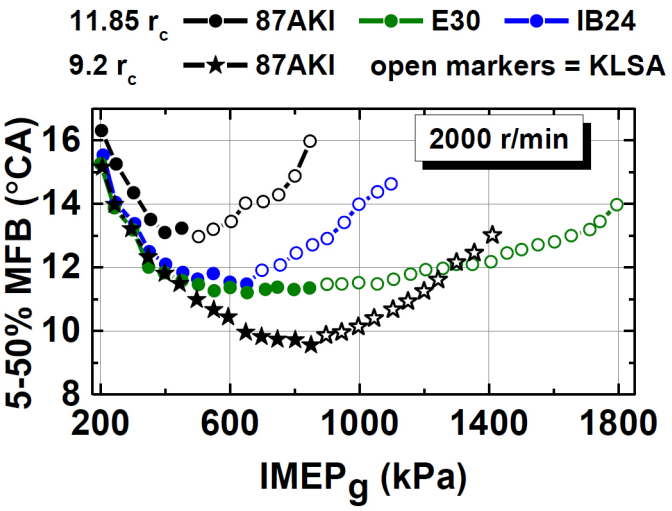

Figure 8. 5-50% MFB duration vs. load at 2000 r/min 0% EGR

The results demonstrate that the production 9.2 r_c piston yields the fastest MFB rates. Based on the findings of Figures 6, 7 and 8, it is reasonable that for 87AKI, the shorter combustion duration with 9.2 r_c enables KLSA CA50 phasing retard to be more effective at mitigating knock than with 11.85 r_c, expanding the $IMEP_g$ in the knock limited regime.

Besides faster combustion duration, the findings of Figure 8 show that as load increases the combustion duration decreases up to the point of knock, where after KLSA phasing results in increasing the combustion duration. Interestingly, E30 retains a fast 5-50% MFB time for most of the KLSA regime. This would help to prevent time-temperature increases and thus knock. This in addition to the HoV findings of Stein et al. [7], aid in increasing the effectiveness of E30 CA50 phasing retard in reducing knock, as seen in Figure 7.

Additionally, previous combustion analysis work by Broustail et al. [21], shows ethanol/isooctane and n-butanol/isooctane mixtures exhibit faster laminar burning velocities than isooctane. Although that work used n-butanol/isooctane mixtures, research by Liu et al. [22] shows that iso-butanol and n-butanol have comparable flame speeds. These cited studies demonstrate that the fundamental burning characteristics of alcohol and gasoline-like fuels differ, where alcohol fuels tend to have shorter combustion duration. Unlike the highly controlled laboratory experiments used to measure laminar burning velocities, internal combustion engine operation generates a wide variety of the conditions. Figure 9 displays the 5-50 MFB time as a function of CA50 under KLSA operation. Note that the same averaging technique used in Figure 7 is applied to the trends in Figure 9.

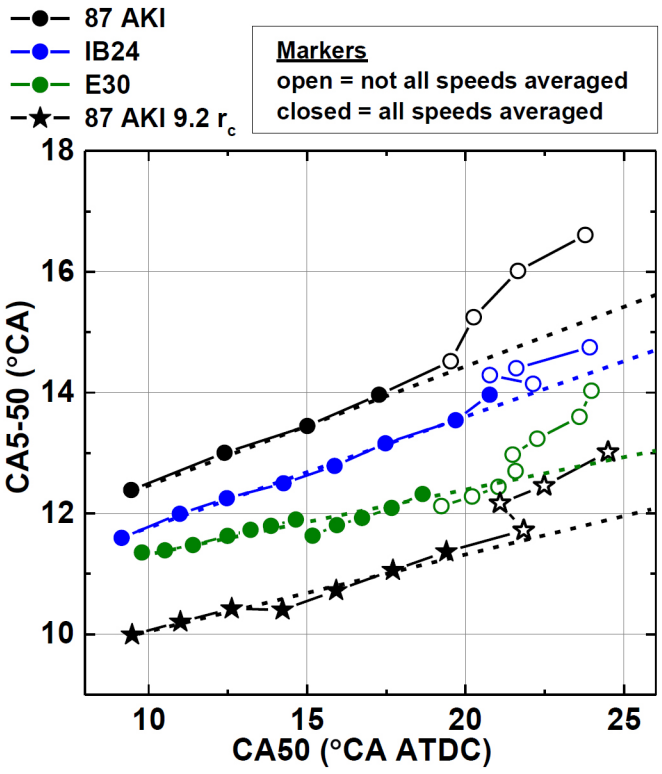

Figure 9. Average of all speeds KLSA 5-50% MFB duration vs. CA50 phasing, solid markers denote all speeds could be averaged, open markers denote less than all speeds could be averaged.

For a given compression ratio, the results in Figure 9 generally correlate with the cited fundamental burning velocity studies. Although the results are plotted as functions of phasing, where the loads differ significantly between fuels and compression ratios, Splitter and Szybist [20] showed that flame speed of intermediate alcohol-gasoline fuels is a function of fuel properties alone and not operating conditions. In that work, E30 was prematurely retarded to match the load and phasing of lower octane number octane fuels (87AKI and IB24), resulting in the knock limited MFB rates being highly dependent on fuel composition, with no correlation to MFB rate and load. Based on the cited works, these results exhibit fuel specific differences, that can be easily overshadowed by combustion chamber design differences. As r_c increases, attention to detail and optimization of the geometry and fluid mechanics may be critical for performance.

MEASURED EFFICIENCY AND EMISSIONS DIFFERENCES

Similar to the observable differences in MFB rates of the production 9.2 r_c piston and the modified 11.85 r_c pistons, observed differences are found in the emissions and efficiency of the two pistons. Figure 10 illustrates the differences in energy budget for the various fuels and compression ratios. In the figure fuel energy is portioned into gross thermal efficiency (GTE), and losses of exhaust (EXH) incomplete combustion (Inc. Comb.) and unaccounted for portions. The latter loss is representative of all energy not directly measured, which encompasses heat transfer. The method used to calculate the losses is discussed in detail in Splitter et al. [36]. Note that an uncompensated[5] FID detector is used for all HC emissions measurements. Kar and Cheng [37] have shown that relative to gasoline exhaust, ethanol containing fuels tend to have disproportionately high ethanol and partially oxidized fuel emissions (i.e., aldehydes). It is well known that ethanol and oxygenated exhaust gas species, like formaldehyde, tend to have low or negligible FID response factors. Thus, to more accurately measure FID based total HC emissions with ethanol containing fuels, the exhaust species mole fractions are required to be known a priori through a detailed chemical speciation. The present study lacks a detailed exhaust speciation, thus the HC emissions of IB24 and E30 are not corrected for FID response. Correction would change the magnitudes of incomplete combustion and heat transfer, but the general trends would remain unaltered.

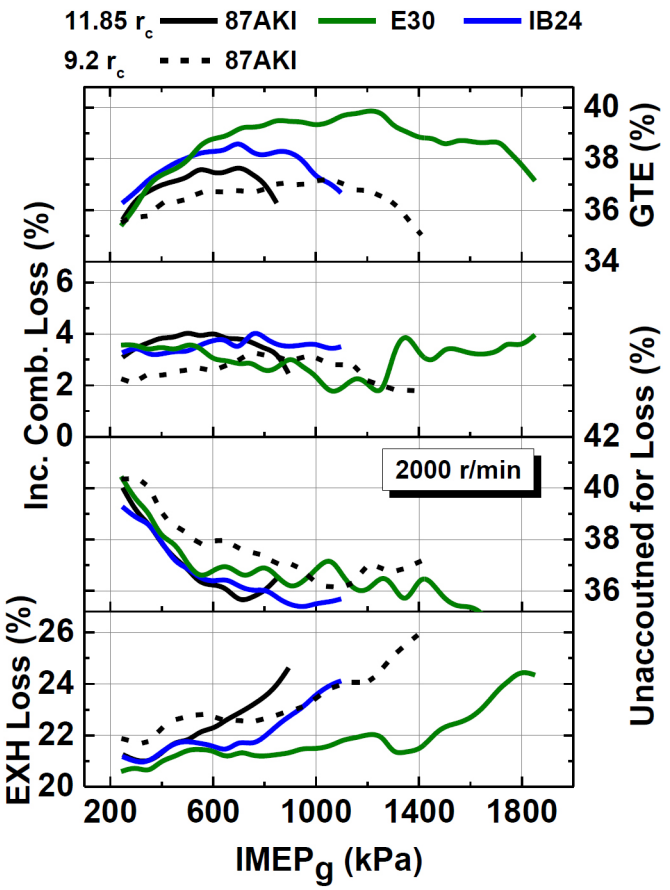

Figure 10. Associated gross based energy budget as a function of load for 2000 r/min operation.

The results of Figure 10 display the expected; the GTE of the lower compression ratio piston is lower than the higher compression ratio piston. However, an interesting finding is that incomplete combustion losses are lower with the 9.2 r_c piston than with the higher compression ratio 11.85 piston (regardless of fuel type for most conditions, i.e., HC FID correction).

The magnitude of the differences in efficiencies and losses between compression ratios are best seen in a direct comparison of the 87AKI gasoline results with the two different compression ratios and with 15% external EGR. These conditions are compared in Figure 11, where all data were at a 500 kPa $IMEP_g$ 2000 r/min operating point, the highest MBT phasing load at 2000 r/min with all three 87AKI strategies.

The results depict incomplete combustion losses of the 9.2 r_c piston are half of those with the 11.85 r_c piston, at matched load-speed condition with the same fuel. Likewise the thermal losses from the lower compression ratio piston are the highest and work (efficiencies) is the lowest.

5 Instrument species response unaltered from that of gasoline

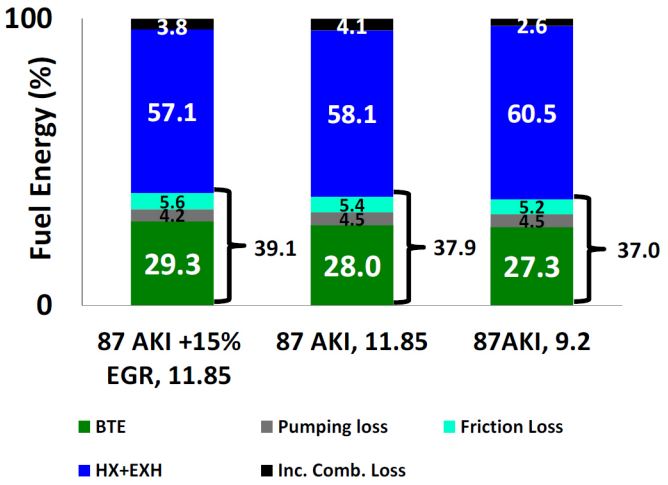

Figure 11. Energy budget for 87AKI gasoline with different EGR and compression ratios. Note that all strategies are at matched CA50 timing of 8°CA ATDC, MBT.

The results of Figures 6, 7, 8, 9, 10, 11 illustrate that the combustion process of the 9.2 r_c piston may be more optimized, thus offering improved combustion attributes even though the efficiency it obtains is reduced. This may bias the higher compression ratio results to lower efficiencies more than a true direct comparison. The direct sources of the specific differences of incomplete combustion losses and MFB rates are beyond the scope of the present study. However, Reitz and Kuo [38] shows that ring pack flow mass increases with higher compression ratio, which Alkidas [39] demonstrated to lead to increased incomplete combustion losses. Additionally, Alkidas [39] stated that in-cylinder fluid mechanics affect incomplete combustion differences. While, geometric factors have been shown by Mattavi [40], and Poulos and Heywood [41] to critically affect MFB rates. Based on these previous findings, it is inferred that as the combustion chamber shape and clearance is altered with the higher compression ratio, differences in turbulence processes, ring pack flows, and MFB rates can occur that critically affect combustion completeness and rate. Regardless of the individual sources, the total effect is that the combustion characteristics of the higher compression ratio piston are less favorable than the lower compression ratio production piston, which may be partly attributed to the increase compression ratio and partly to a less engineered design.

The MFB and emissions discrepancies between the pistons make isolating compression ratio effects less direct. For example, increased MFB rate can decrease end gas knock, as the time-temperature history of the end gas is reduced. In the present experiment, there was a direct comparison of operating conditions between fuels and compression ratios. Although beyond the scope of the present study, there potentially may be optimization opportunities of components and calibration to further the performance and reduce emission of the different fuels at either compression ratio. However, it is desirable to gauge the amount of theoretical efficiency unutilized by the higher compression ratio piston, determining the upper bound what further optimization may enable.

To estimate the theoretical maximum upper bound gain in cycle efficiency, the standard air (Otto) cycle efficiency of the different pistons and EGR rates was calculated, as defined in Eq. 1.

$$\eta_{thermal} = 1 - \left(\frac{1}{r_c^{(\gamma-1)}}\right) \quad (1)$$

Equation 1 is a function of only the compression ratio and gamma (the ratio of specific heats). Due to non-idealities in actual engine operation, such as heat transfer, Eq. 1 is less useful for quantitative prediction of efficiency, but can be used as a qualitative estimation method for comparing the theoretical (upper bound) performance differences in working fluid properties (gamma) and compression ratio.

Assuming ideal gas behavior, gamma is a function of temperature only. During fired operation, gamma of the working fluid is reduced after combustion through changes to both temperature and chemical composition. The present analysis applies Eq. 1 using an average of the compression and expansion gamma,[6] each determined from the ensemble average pressure data. Using this approach, a comparison of the theoretical and measured efficiencies is made.

The theoretical maximum efficiencies of the data in Figure 11 are calculated. The calculated average gammas used, and corresponding theoretical and measured gross thermal efficiency differences, are presented in Table 4.

Table 4. Measured and predicted Otto cycle efficiencies relative to 500 kPa IMEPg for 87AKI 11.85 r_c 0% EGR operation.

	11.85 r_c 15% EGR	11.85 r_c 0% EGR	9.2 r_c 0% EGR
Measured average gamma (-)	1.31	1.30	1.30
Maximum theoretical η gain vs. 11.85 r_c 0% EGR (-)	+ 0.4	NA	- 3.8
Measured η gain vs. 11.85 r_c 0% EGR (-)	+1.2	NA	-0.9

6 Gamma determined from the log of pressure vs. volume during the linear portion of the compression stroke

If all other factors remained equal, the difference in Table 4 should be directly reflected in the GTE of the two strategies. However, the measured gain in the efficiency row illustrates that the idealized assumptions used in Eq. 1 are not achieved in application. For example, the incomplete and thermal losses in Figure 11 affect the measured efficiencies. The results show that the measured efficiency was better than predicted with EGR and lower than predicted with the lower compression ratio.

Although the approach used averages the expansion and compression gamma, it retains the logical trends in that gamma is a function of composition and temperature alone. The reduction in gamma with 0% EGR is attributed to compositional differences with stoichiometric gasoline-air mixtures and EGR [19]. For the different compression ratios of expansion and compression gammas with lower compression ratio compete, due to lower temperature on compression, raising gamma, but higher temperature during expansion (Figure 10) reducing gamma, yielding a zero net difference in gamma from the higher r_c piston.

From Table 4 it is clear that the difference in GTE between the 11.85 and 9.2 r_c pistons is only 0.9 percentage points. This was approximately $1/4^{th}$ of the theoretical maximum difference (3.8%), with the 11.85 r_c piston. Figure 11 illustrates that additional incomplete combustion losses are present with the 11.85 r_c piston. To bound the realizable magnitude of these additional losses can have on efficiency, the following was computed: At the measured 37.9% GTE, the 1.5% increase in incomplete combustion between the 9.2 and 11.85 r_c pistons corresponds to a realizable GTE difference of approximately 0.5% (1.5%*0.379). Thus, the difference in GTE of the measured vs. predicted values in Table 4 would have made the measured gain in GTE −1.4 instead of −0.9, had the pistons had identical incomplete combustion losses, and all combusted fuel went to work at the measured GTE level. Therefore, even with matched incomplete combustion losses, the achieved GTE of the 11.85 r_c piston was still approximately half of the theoretical gain relative to the 9.2 r_c piston, demonstrating that non-ideal factors can affect real engine efficiency beyond those predicted by an Otto analysis. This analysis demonstrates there is effectively much less of a difference in GTE that is practically achieved with higher compression ratio, thus even with non-idealities a direct comparison of performance between compression ratios is still applicable.

Additionally noted in Figure 11, is that there is higher friction (cyan bars) when the compression ratio is increased. These differences are well understood phenomena as increased compression ratio increases peak cylinder pressure and thus bearing squeeze film friction. In this study friction was correlated, where the approach used is discussed in greater detail in the following section. Likewise, in Figure 11, the difference in efficiency with 15% and 0% external EGR (left and center bars) was similar to other reported data [19]. When using 15% external EGR a reduction in exhaust temperature occurs, and thus exhaust losses. Additionally, pumping losses decrease because added diluent mass raises intake pressure and reduces intake throttling.

CALCULATED BRAKE PERFORMANCE DIFFERENCES

The present analysis demonstrates that there are fuel and combustion design differences that are measured on an indicated basis. Although indicated data is useful for understanding detailed combustion phenomena, it is desirable to estimate the performance under real engine operation. It is common to use friction correlations from single-cylinder engines to estimate the performance of a multi-cylinder design. This approach is used in the present study where the brake mean effective pressure (BMEP) and corresponding brake thermal efficiency (BTE) of the tested fuels and compression ratios are calculated. The calculation uses the GTPower friction mean effective pressure (FMEP) correlation with the default constant values [42]. Further details on the approach can be found in Splitter and Szybist [43]. The correlation is calculated using Eq. 2, which is a function of peak cylinder pressure (PCP), mean piston speed ($\bar{P}_s$), and of four constants (C1-C4); with the applied constant values in Table 5.

$$FMEP = C_1 + (C_2 * PCP) + (C_3 * \bar{P}_s) + \left(C_4 * \bar{P}_s^{\,2}\right) \quad (2)$$

Table 5. FMEP constants used in this study.

C_1 (bar)	0.04
C_2 (bar)	0.005
C_3 (bar)	0.09
C_4 (bar)	0.0009

Using the stated correlation and constants, the BTE and BMEP of all fuels are calculated. Figure 12 presents the correlated BMEP and BTE at a 2000 r/min operating speed with the different fuels, compression ratios, and EGR levels.

The results demonstrate that both fuels and EGR can improve BTE, with all fuels displaying BTE benefits with 15% EGR. The comparison below approximately 200 kPa was omitted because the difference in BTE was small as all strategies are heavily throttled for λ=1 operation.

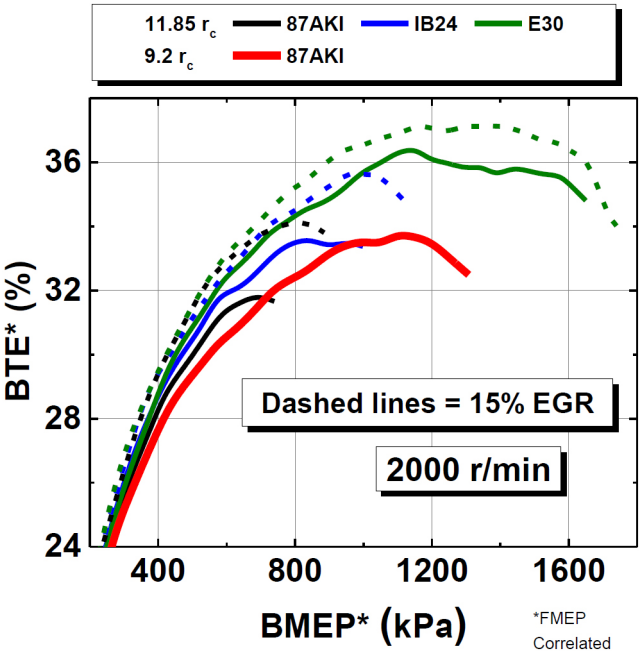

Figure 12. Estimated BTE and BMEP of all fuels and EGR rates tested at 2000 r/min.

Steady State Vehicle MPG Estimates

As stated in the introduction, the evolutionary progression of the internal combustion engine has led to smaller displacement and higher power/torque density engines. However to meet mandated CAFE standards and RFS II quota, higher octane bio-fuels may be enabling technologies. So long as MPG can remain similar to conventional distillate fuels, the potential benefits are assessed using a representative vehicle road load and highway cruise analysis in this and the following sub-section.

As indicated in Figure 12, EGR use should be considered to maximize engine BTE. Although BTE is a convenient comparison, it does not account for volumetric energy density differences between fuels. To include volumetric energy density differences, a relative BTE for a given fuel was compared in the present analysis. For all comparisons, a baseline condition of 87 AKI 9.2 r_c with 0% EGR was used (as estimate of the stock engine). The relative BTE to the baseline condition was calculated using Eq. 3.

$$relative\ BTE = 100 * \left(\frac{BTE_{xx} - BTE_{87AKI\ 9.2\ r_c}}{BTE_{87AKI\ 9.2\ r_c}}\right) \quad (3)$$

Unlike absolute BTE difference, the relative BTE difference determines the relative difference between given strategies from another. Using this manner of comparison is more convenient as it shows the amount that BTE has improved relative to a given strategy, and thus can be used to account for the relative differences in volumetric fuel energy. For example, Table 6 displays the differences in volumetric energy and corresponding required relative BTE for matched MPG between E30, IB24 to 87AKI and an estimated E10[7] (conventional gasoline), all differences calculated using the properties from Table 3.

Table 6. Difference in volumetric fuel energy of tested intermediate alcohol-gasoline blend fuels compared to E0 or E10 gasoline.

	E30 vs. E0	E30 vs. E10	IB24 vs. E0	IB24 vs. E10
fuel energy Δ per unit volume (%)	-10.4	-7.2	-4.2	-0.9
relative BTE Δ (%) at matched MPG	-10.4	-7.2	-4.2	-0.9

Note that the values of Table 6 demonstrate that the fuel energy difference and relative BTE difference are synonymous. Thus, a direct estimate of the difference in MPG between the different fuels can be made through the relative BTE difference. This approach is used between conventional fuels and intermediate alcohol fuels in Figures 12 and 13, which display the relative BTE between 11.85 r_c E30+15% EGR vs. 9.2 r_c 87 AKI, and 11.85 r_c IB24+15% EGR vs. 9.2 r_c 87 AKI respectively.

Additionally, in both Figure 12 and 13, two grey lines labeled 1.2L and 2.0L are overlaid. These indicate a line of a constant 16 kW power, the road load for a typical U.S. midsize MY2012 sedan at 65 MPH steady cruise, as determined from EPA chassis dynamometer data [44].The lines are four points labeled A, B, C, and D, which denotes generic operating conditions for various engine and transmission configurations, listed in Table 7. Note that the same MPG estimation approach was used in Splitter and Szybist [43], which showed very good agreement between MPG estimates correlated from steady-state engine experiments and EPA chassis dynamometer road load coefficients vs. production vehicle steady state chassis dynamometer measured MPG.

Table 7. Downsize and Downspeed Configurations.

Condition	A	B	C	D
40% Downsize	-	-	X	X
36% Downspeed	-	X	-	X

7 E10 LHV and density estimated from the measured fuel properties in Table 3.

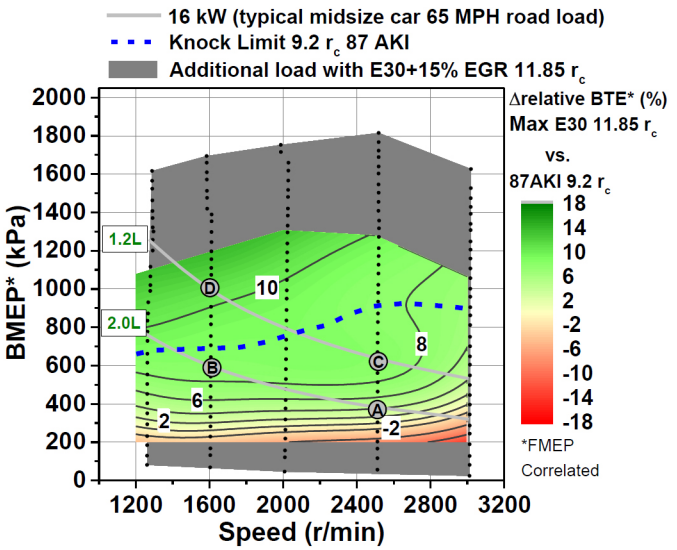

Figure 13. Estimated map of relative BTE for 11.85 r_c E30+15% EGR vs. 9.2 87AKI 9.2 r_c, including 65MPH steady cruise road load for conditions A-D described in Table 7.

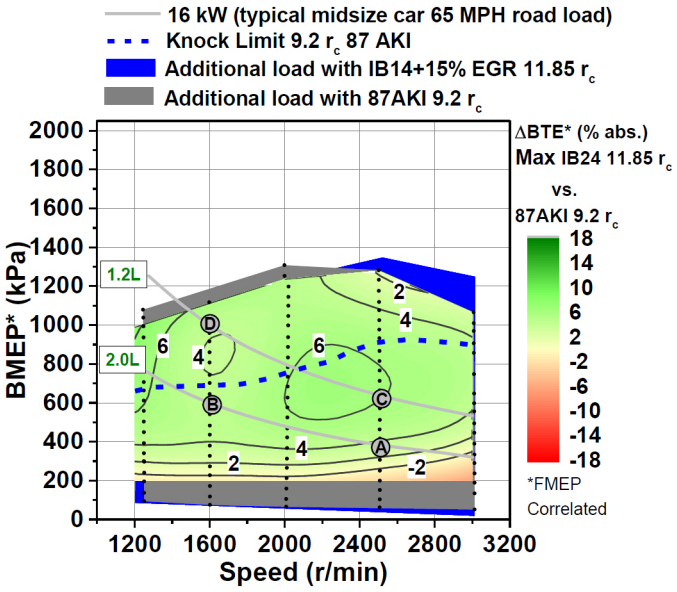

Figure 14. Estimated map of relative BTE for 11.85 r_c IB24+15% EGR vs. 9.2 87AKI 9.2 r_c, including 65MPH steady cruise road load for conditions A-D described in Table 7.

The results displayed in Figures 12 and 13 show that, for either E30 or IB24 for loads above approximately 300-400 kPa, intermediate biofuels +15%EGR can achieve equivalent or better MPG than 87AKI 9.2 r_c operation. The comparison data was not shown at loads below 200 kPa, because the absolute BTE was small, which can cause the relative BTE difference to be magnified beyond what may be reasonable. Note that that at loads below 200 kPa, the alcohol fuels underperformed E0 gasoline by a marginal amount.

The trends in the figures illustrate that for most loads the intermediate biofuels operating with the higher compression ratio piston are equivalent or better than E0 gasoline. Additionally, IB24+15% EGR was found to have a near identical load-speed map to 87AKI with 9.2 r_c, but was found to offer marked MPG and correspondingly CO_2 emissions improvement potential.

Since the higher compression piston was non-optimized, the potential for further improvements or relaxation of EGR requirement for high r_c E30 breakeven MPG may be possible. These findings are similar to those shown by Jung et al. [13], which demonstrate that intermediate alcohol-gasoline bio-fuels can achieve equivalent MPG to conventional distillate fuels with different higher r_c engines.

Downsize + Downspeed merit

Figures 13 and 14 demonstrate that the benefits of intermediate alcohol-gasoline blends, specifically E30, can offer comparable performance to gasoline for loads above approximately 300-400 kPa, and IB24+15% EGR with a 2.65 point increase in r_c can match the load-speed range with decreased MPG compared to 87AKI. These findings suggests that a given powertrain (engine and transmission) combination can yield similar or better MPG with bio-fuels. Additionally for E30, the equivalent MPG but increased maximum torque limit may enable different optimal powertrain and compression ratios designs.

The present sub-section builds on the steady state MPG comparisons of Figures 13 and 14 by estimating the performance of the presented two generic engine and transmission configurations (Table 7), using a factorial approach of downsized and downspeed configurations at a 65 MPH steady cruise condition. This analysis uses steady state engine data, with simulated boost and friction, requiring significant assumptions. Therefore, the following analysis is for illustrative purposes only and is not representative of production intent designs that may require turbocharger matching, launch ability, acceleration, multi-speed transmissions and shift point optimization etc.

Others have shown that a major factor in extreme downsizing is boost system response. For example, Fraizer et al. [45] indicated that in ultra-downsized engines both engine and boost systems need to be designed to achieve high power and torque. Both that work and Bozza et al. [46] showed a multi second lag in turbocharger response in downsized and downspeed engines. More recently, Keidel et al. [47] demonstrated that in the high boost and shift frequency demands of heavy-duty trucks, a split boosting strategy with a turbocharger augmented by a clutched supercharger may enable very good transient response in configurations that are downsped by over 25% (400 r/min in heavy-duty engine). A similar system was shown in a light-duty sized engine in a low-temperature combustion concept to add great benefit and

provide very fast boost response by Hoyer et al. [48] in a prototype engine, and more recently in a production viable multi-cylinder variant by Sellnau et al. [49].

These cited works suggest that with proper engineering, systems design, and integration, extreme downsized engines may become more possible. The present analysis uses steady state operation to explore the fundamental effects of fuels and knock in extreme downsizing and downspeeding (~36%) to estimate if fuels are enabling technologies for increasing vehicle MPG. Note that in the present analysis a production intent downsized downsped engine at least requires consideration of the above cited system-level components and designs, along with significant design-specific engineering, all of which are beyond the present scope. Regardless, the utility of the present analysis is that it demonstrates if merit for investigating the transient response exists for a specific fuel and compression ratio in a downspeed and downsize powertrain application. Figures 13 and 14 demonstrate that the relative improvement in BTE is very similar at conditions A and C ("standard" transmission, i.e., not downsped). Although the relative BTE was flat, the absolute BTE does improve with downsizing (Conditions C vs. A). This information is masked in the relative BTE comparison of Figures 13 and 14. Figure 15 displays the absolute BTE for 87KI 9.2 r_c operation.

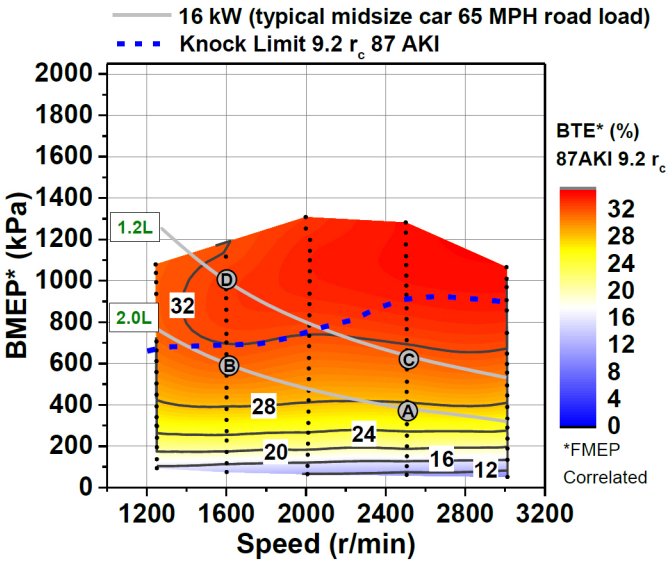

Figure 15. Estimated BTE contours for 9.2 r_c 87AKI gasoline, including 65MPH steady cruise road load for conditions A-D described in Table 7.

The figure illustrates that the BTE of Conditions B and C are almost identical, approximately 4 points higher than that of the baseline conditions (condition A). However because the powertrain is downsped 36% at condition B or downsized by 40% at condition C, the fuel consumption differences between conditions B and C are minimal. Likewise, both conditions exhibit similar reserve torque (torque difference from condition to maximum load). Due to these similarities, data at condition C is not used in the following analysis.

Using conditions A, B, and D of Table 7, the steady cruise MPG incentive for the downspeed designs with a 2.0 and 1.2L engine (B and D respectively) are presented in Figure 16

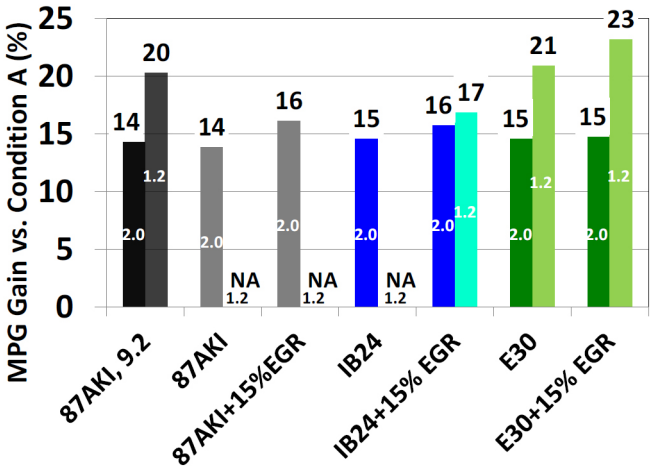

Figure 16. Relative gain in MPG with downspeeding from 2500 r/min to 1600 r/min with and without downsizing (1.2L vs. 2.0L engine displacements). Relative MPG values are denoted atop each column with engine displacement denoted in the column center (2.0 or 1.2 L engine).

The results depict that there is a relatively constant 15% improvement in MPG vs. the baseline condition (condition A) if the baseline 2.0L engine is downsped, and between 17% and 23% improvement in MPG if the powertrain is downsized and downsped (1.2L engine). Note that the MPG gain values in Figure 16 are relative to the given fuel and not to the baseline condition of 9.2 r_c 87AKI gasoline.

The results further illustrate with a 40% downsizing the engine from a 2.0L to a 1.2L, E30 and 11.85 r_c and 87AKI with 9.2 r_c offer the most MPG benefit potential. This is interesting as a simple downspeeding offers near identical MPG benefit with all fuels, compression ratios, and EGR rates. The results show that there is more volatility, and even incompatibility (i.e., 87AKI and IB24 11.85 r_c), in the MPG benefit with downsize + downspeed design (condition D). This is undesirable as the compatible fuels at condition D yield the highest relative MPG gain to the baseline powertrain (condition A) offering the best potential to meet future CAFE standards.

The reason for the added volatility with the downsize + downspeed powertrain is that for some fuels there is heavy KLSA at condition D (1000 kPa BMEP, 1600 r/min). Figure 17 illustrates the CA50 phasing for both downspeed conditions B (2.0L) and D (1.2L).

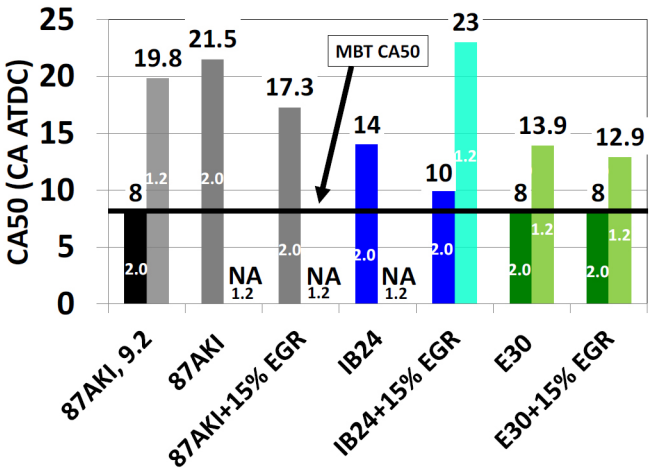

Figure 17. CA50 combusiton phasing for all tested fuels, compression ratios, and EGR rates at conditions B and D of Table 7. Column values are denoted atop each column with engine displacement denoted in the column center (2.0 or 1.2 L engine).

The results exhibit that relative to the other fuels, EGR rates, and compression ratios the phasing retard with E30 is significantly reduced. This is of particular interest. Recall from Figure 5 that 87AKI 9.2 r_c and E30 11.85 r_c enter KLSA operation at the same load-speed point, yet the phasing of 87AKI was much more retarded after entering KLSA. These results indicate that there likely are fuel specific considerations when considering the next generation downsized + downspeed powertrain designs.

The aggressive retard with 87AKI and IB24 becomes most apparent when the reserve torque at the downspeed conditions B and D are examined (1600 r/min for the 2.0L and 1.2L designs). The results of the analysis are plotted in Figure 18.

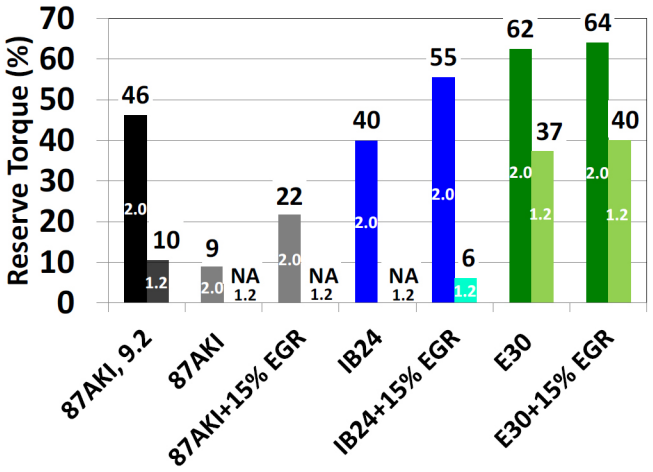

Figure 18. Reserve torque for all tested fuels, compression ratios, and EGR rates at conditions B and D of Table 7. Column values are denoted atop each column with engine displacement denoted in the column center (2.0 or 1.2 L engine).

The results of Figures 14, 15, 16 illustrate the trends in MPG, KLSA, and λ=1 reserve torque are intimately intertwined, requiring simultaneous optimization and consideration. Although there are significant MPG advantage to move towards excessive downsized + downspeed powertrain designs (condition D in this analysis), the combustion phasing and reserve torque are very fuel and compression ratio specific. The results show that E30 with or without EGR in a downsized + downsped configuration enables nearly the same reserve torque as 87AKI with 9.2 r_c (the stock engine configuration). The results effectively establish that the more aggressive KLSA retard requirement of 87AKI and IB24 reduce the downsizing and downspeeding options relative to E30.

Finally to combine the trends of MPG and reserve torque with downsizing and downspeeding, a merit function was defined. Equation 4 describes the function, which is used to determine the amount of observed difference in MPG vs. the reduction in reserve power.

$$Downsize\ Merit = \frac{\%\ gain\ in\ MPG}{\%\ Loss\ in\ reserve\ power} - 1 \quad (4)$$

Using Eq. 4, the downsize merit of downsizing + downspeeding (condition D) is compared to downspeeding (condition B), to assess if downsizing is of merit in a downspeed configuration. The results from the merit function comparison are plotted in Figure 19.

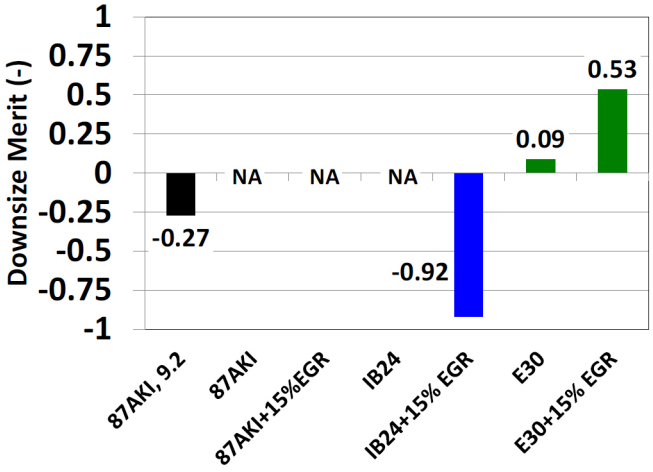

Figure 19. Downsize merit for all tested fuels, compression ratios, and EGR rates using Eq. 4 for conditions D relative to condition B from Table 7.

The data demonstrates that E30 was the only fuel and EGR combination that had a greater increase in MPG vs. loss in reserve power at the downsized + downsped vs. downspeed condition. This finding suggests that the benefits for downsizing + downspeeding with intermediate ethanol-gasoline fuels may be different and more beneficial than those of conventional gasoline or other alcohol-gasoline blends, offering merit to future studies to investigate the production feasibility of more extreme downsized and downspeed powertrains.

Discussion

The present study validates that improvements to the base engine design may be enabled if mid-level alcohol-gasoline blends like IB24 and E30 are to be used as a future fuels. Specifically, E30 demonstrates improved anti-knock tendencies beyond the values defined by the RON and MON tests. The less aggressive KLSA demand of E30 offers significant advantages in load expansion. Both engine efficiency and load are furthered with 15% external EGR, which may be more common on future engines. To best capitalize on the benefits, the engine may need to be optimized to take advantage of the higher r_c and KLSA load space. The results demonstrate that the use of mid-level alcohol blends, such as E30, may open the door to extreme engine downsizing with the potential for λ=1 operation. If pursued, extreme downsizing may require changes to the engine beyond those investigated in the present study, specifically to air handling and transmission gear number and shift points.

For example, transient response of air handling system(s) and the associated higher mass flow rate of air per unit displacement may require base engine and air handling optimization. These tradeoffs and optimization may be more involved with the inclusion of external EGR. Likewise, heat transfer effects may be of greater importance in downsized platforms as surface to volume relations scale as the square and cubic of bore radius respectively. The present study has ignored these dimensional effects that may be present in application. However, the present findings demonstrate the general trends that could be expected with thorough and proper engineering of the base engine and supporting systems.

The focus of the present study is on engine efficiency, so a compression ratio of 2.65 points higher than stock is used (11.85:1 vs. 9.2:1). Of course this biases the results towards higher octane fuels, but these combinations may be required to meet imposed CAFE standards in conjunction with the RFS II standards. The results validate that as compression ratio is increased, the combustion chamber shape can affect MFB rates, and thus attention to detail must be performed to help to retain fast burning rates. If executed properly, advancement of engine design and powertrain options may be enabled with simultaneous RFS II adoption. This presents a unique and infrequent opportunity to dramatically alter internal combustion engine operation from improving fuel properties.

CONCLUSIONS

The findings of this study are applicable to SI engine fuel economy and performance. Specifically, two mid-level alcohol blends are compared to regular pump gasoline (87AKI) that had 0% ethanol. The fuels were compared with 0% and 15% EGR at five speeds from 2 bar $IMEP_g$ to a full load condition, where either a combustion phasing or an EGT limit is met. The results demonstrate that E30 offered the highest stoichiometric torque capability at high compression ratio.

A detailed combustion analysis is performed with all fuels. The results illustrate several findings. Most notably the load expansion possible with intermediate alcohol-gasoline bio-fuels is not well indicated by the octane number tests. E30 displayed significant knock limited load increase, with little combustion duration sensitivity to combustion phasing. Although the intermediate alcohol fuel displayed the fastest combustion durations and least phasing retard in knock limited operation, combustion chamber geometry and optimization are critical, and incomplete combustion losses and turbulence effects need to be considered when increasing compression ratio. The trends show that with the higher compression ratio piston, incomplete combustion losses are doubled. MFB rate differences are observed between the fuels with given compression ratio, where E30 and IB24 offered faster 5% to 50% MFB times than 87AKI. However, the stock 9.2 r_c piston yield the fastest MFB times, demonstrating that combustion chamber optimization is very important, and poorly designed combustion chamber can more than offset improvements by fuel properties alone.

The combustion analysis of KLSA operation is linked to differing powertrain options. Specifically, E30 11.85 r_c and 87AKI 9.2 r_c enter KLSA operation at the same speed-load condition, but the KLSA load is approximately twice as large with E30 than 87AKI. This had positive implications on E30 lending itself to be potentially better suited for further downsized and downspeed powertrain configurations. Likewise in a steady state analysis of a ~40% downsized + downspeed powertrain E30 is found to offer improvements to MPG at a faster rate than a decrease in reserve torque, suggesting that more extreme engine downsizing and downspeeding may be possible with intermediate ethanol-gasoline fuels.

The combined findings depict that mid-level ethanol blends offer more than high RON and MON and HoV values, in that they can exhibit improved combustion and knock mitigation phenomena, especially with mid-level ethanol blends like E30. If increases in engine efficiency are the vehicle engine technology pinnacle strived for, then changes to the fuel infrastructure through mid-level alcohol blends may be enabling steps to feasible, near-term increases in vehicle efficiency.

CONTACT INFORMATION

Derek Splitter
splitterda@ornl.gov

Jim Szybist
szybistjp@ornl.gov

ACKNOWLEDGMENTS

The authors gratefully acknowledge the support of the U.S. Department of Energy, particularly Kevin Stork and Steve Przesmitzki of Office of Vehicle Technologies. Additionally, the authors would like to acknowledge John Thomas for his assistance with road load calculations, and Vicki Kalaskar for assistance with the engine test laboratory.

DISCLAIMER

DEFINITIONS/ABBREVIATIONS

AFR - air fuel ratio

AKI - anti-knock index

ATDC - after top dead center

BOB - blendstock for oxygenate blends

BTE - brake thermal efficiency

CA - crank angel

CA50 - crank angle of 50% mass fraction burned

CAFE - corporate average fuel economy

CO - carbon monoxide

CO2 - carbon dioxide

DI - direct injection.

E0 - zero percent ethanol

E10 - ten percent ethanol

E30 - thirty percent ethanol

EGR - exhaust gas recirculation

EGT - exhaust gas temperature

EPA - Environmental Protection Agency

EXH - exhaust

FID - flame ionization detector

FSN - filter smoke number

GTE - gross thermal efficiency

HC - hydrocarbon

HoV - enthalpy of vaporization.

HRR - heat release rate

HVA - hydraulic valve actuation.

IB24 - twenty four percent iso-butanol

$IMEP_g$ - gross indicated mean effective pressure

Inc. Comb - incomplete combustion

KLSA - knock limited spark advance

LD - light-duty

LHV - lower heating value

MBT - maximum brake torque

MFB - mass fraction burned

MON - motor octane number.

MPG - miles per gallon

NA - not applicable

NHTSA - National Highway transportation and Safety Administration

NOx - nitrogen oxide emissions

$\bar{P}_s$ - mean piston speed

PCP - peak cylinder pressure

r_c - Compression raito

RFS II - Renewable Fuel Standards Two

RON - research octane number

S - fuel octane sensitivity

SI - spark ignition.

U.S. - United States

VVA - variable valve actuation

γ - gamma

η - efficiency

λ - lambda

REFERENCES

1. One Hundred Tenth Congress of the United States of America, Energy Independence and Security Act of 2007. 2007; H.R. 6.
2. Environmental Protection Agency, “40 CFR Part 80 Regulation of Fuels and Fuel Additives: 2011 Renewable Fuel Standards; Final Rule”, available at, http://www.gpo.gov/fdsys/pkg/FR-2010-12-09/pdf/2010-30296.pdf, accessed May 2, 2013.
3. Energy information agency transportation sector energy consumption report, http://www.eia.gov/totalenergy/data/monthly/#consumption, accessed May 2, 2013.
4. National Highway Traffic Safety Administration and Environmental Protection Agency, “2017 and Later Model Year Light-Duty Vehicle Greenhouse Gas Emissions and Corporate Average Fuel Economy Standards; Final Rule” available at http://www.nhtsa.gov/fuel-economy, accessed May 2, 2013.
5. Environmental Protection Agency, “Light-Duty Automotive Technology, Carbon Dioxide Emissions, and Fuel Economy Trends:1975 Through 2012”, available at, http://www.epa.gov/fueleconomy/fetrends/1975-2012/420r13001.pdf, accessed May 2, 2013.
6. Fraser, N., Blaxill, H., Lumsden, G., and Bassett, M., “Challenges for Increased Efficiency through Gasoline Engine Downsizing,” *SAE Int. J. Engines* 2(1):991-1008, 2009, doi:10.4271/2009-01-1053.
7. Stein, R., Polovina, D., Roth, K., Foster, M. et al., “Effect of Heat of Vaporization, Chemical Octane, and Sensitivity on Knock Limit for Ethanol - Gasoline Blends,” *SAE Int. J. Fuels Lubr.* 5(2):823-843, 2012, doi:10.4271/2012-01-1277.
8. Stein, R., House, C., and Leone, T., “Optimal Use of E85 in a Turbocharged Direct Injection Engine,” *SAE Int. J. Fuels Lubr.* 2(1):670-682, 2009, doi:10.4271/2009-01-1490.
9. Szybist, J., Foster, M., Moore, W., Confer, K. et al., “Investigation of Knock Limited Compression Ratio of Ethanol Gasoline Blends,” SAE Technical Paper 2010-01-0619, 2010, doi:10.4271/2010-01-0619.
10. Szybist, J.P., Chakravathy, K., Daw C.S., “Analysis of the Impact of Selected Fuel Thermochemical Properties on Internal Combustion Engine Efficiency” Energy & Fuels, Volume: 26 Issue: 5 Pages: 2798-2810 DOI:10.1021/ef2019879 Published: MAY 2012.

11. Stein, R., Anderson, J., and Wallington, T., "An Overview of the Effects of Ethanol-Gasoline Blends on SI Engine Performance, Fuel Efficiency, and Emissions," *SAE Int. J. Engines* 6(1):470-487, 2013, doi:10.4271/2013-01-1635.
12. Jung, H., Shelby, M., Newman, C., and Stein, R., "Effect of Ethanol on Part Load Thermal Efficiency and CO_2 Emissions of SI Engines," *SAE Int. J. Engines* 6(1):456-469, 2013, doi:10.4271/2013-01-1634.
13. Jung, H., Leone, T., Shelby, M., Anderson, J. et al., "Fuel Economy and CO_2 Emissions of Ethanol-Gasoline Blends in a Turbocharged DI Engine," *SAE Int. J. Engines* 6(1):422-434, 2013, doi:10.4271/2013-01-1321.
14. Szybist, J. and West, B., "The Impact of Low Octane Hydrocarbon Blending Streams on the Knock Limit of "E85"," *SAE Int. J. Fuels Lubr.* 6(1):44-54, 2013, doi:10.4271/2013-01-0888.
15. Anderson, J.E., Kramer, U., Mueller, S.A., Wallington, T.J., "Octane Numbers of Ethanol - and Methanol - Gasoline Blends Estimated from Molar Concentrations," Energy & Fuels 24(12):6576-6585, 2010, doi:4134154/ef101125c.
16. Anderson, J., Leone, T., Shelby, M., Wallington, T. et al., "Octane Numbers of Ethanol-Gasoline Blends: Measurements and Novel Estimation Method from Molar Composition," SAE Technical Paper 2012-01-1274, 2012, doi:10.4271/2012-01-1274.
17. Foong, T. M., Morganti, K. J., Brear, M. J., da Silva, G., Yang, Y., & Dryer, F. L. (2014). The octane numbers of ethanol blended with gasoline and its surrogates. *Fuel*, 115, 727-739.
18. High Octane Fuel Symposium, International Society of Automotive Engineers, January 2013, Washington, D.C., http://www.sae.org/events/hofs/.
19. Alger, T., Mangold, B., Roberts, C., and Gingrich, J., "The Interaction of Fuel Anti-Knock Index and Cooled EGR on Engine Performance and Efficiency," *SAE Int. J. Engines* 5(3):1229-1241, 2012, doi:10.4271/2012-01-1149.
20. Splitter, D.A., and Szybist, J.P., "An Experimental Investigation of Spark-Ignited Combustion with High-Octane Bio-Fuels and EGR. 2. Fuel and EGR Effects on Knock Limited Load and Speed." *Energy & Fuels* 2013, DOI:10.1021/ef401575e.
21. Broustail, Guillaume, et al. "Experimental determination of laminar burning velocity for butanol and ethanol iso-octane blends." *Fuel* 90.1 (2011), 1-6.
22. Liu, Wei; Kelley, A. P.; and Law C. K. "Non-premixed ignition, laminar flame propagation, and mechanism reduction of< n-butanol, iso-butanol, and methyl butanoate." *Proceedings of the Combustion Institute* 2011, 33.1, 995-1002.
23. Wheeler, J., Polovina, D., Ramanathan, S., Roth, K. et al., "Increasing EGR Tolerance using High Tumble in a Modern GTDI Engine for Improved Low-Speed Performance," SAE Technical Paper 2013-01-1123, 2013, doi:10.4271/2013-01-1123.
24. Alger, T., Gingrich, J., Mangold, B., and Roberts, C., "A Continuous Discharge Ignition System for EGR Limit Extension in SI Engines," *SAE Int. J. Engines* 4(1):677-692, 2011, doi:10.4271/2011-01-0661.
25. Szybist, J., Nafziger, E., and Weall, A., "Load Expansion of Stoichiometric HCCI Using Spark Assist and Hydraulic Valve Actuation," *SAE Int. J. Engines* 3(2):244-258, 2010, doi:10.4271/2010-01-2172.
26. Weall, A., Szybist, J., Edwards, K., Foster, M. et al., "HCCI Load Expansion Opportunities Using a Fully Variable HVA Research Engine to Guide Development of a Production Intent Cam-Based VVA Engine: The Low Load Limit," *SAE Int. J. Engines* 5(3):1149-1162, 2012, doi:10.4271/2012-01-1134.
27. Heywood, J.B., Internal Combustion Engine Fundamentals, McGraw-Hill, 1988.
28. *Federal Register*, Vol. 75(213), Thursday, November 4, 2010, Notices.
29. *Federal Register*, Vol. 76(17), Wednesday, January 26, 2011, Notices.
30. US Environmental Protection Agency proposed ruling, "Control of Air Pollution from Motor Vehicles: Tier 3 Motor Vehicle Emission and Fuel Standards," http://www.epa.gov/otaq/tier3.htm, accessed May 2, 2013.
31. National Renewable Energy Laboratory Report "Utilization of Renewable Oxygenates as Gasoline Blending Components" accessible at http://www.nrel.gov/docs/fy11osti/50791.pdf, accessed May 2, 2013.
32. American Petroleum Institute, Alcohols and Ethers, A Technical Assessment for Their Application as Fuels and Fuel Components, Third Ed., API Pub. 4261, June 2001.
33. Wilhoit, R.C.; Zwolinski, B.J. "Physical and Thermodynamic Properties of Aliphatic Alcohols." Journal of Physical and Chemical Reference Data, Vol. 2, 1973, Supplement No. 1.
34. Leppard, W., "The Chemical Origin of Fuel Octane Sensitivity," SAE Technical Paper 902137, 1990, doi:10.4271/902137.
35. Mittal, V., Heywood, J., and Green, W., "The Underlying Physics and Chemistry behind Fuel Sensitivity," *SAE Int. J. Fuels Lubr.* 3(1):256-265, 2010, doi:10.4271/2010-01-0617.
36. Splitter, D., Wissink, M., DelVescovo, D., and Reitz, R., "RCCI Engine Operation Towards 60% Thermal Efficiency," SAE Technical Paper 2013-01-0279, 2013, doi:10.4271/2013-01-0279.
37. Kar, K. and Cheng, W., "Speciated Engine-Out Organic Gas Emissions from a PFI-SI Engine Operating on Ethanol/Gasoline Mixtures," *SAE Int. J. Fuels Lubr.* 2(2):91-101, 2009, doi:10.4271/2009-01-2673.
38. Reltz, R. and Kuo, T., "Modeling of HC Emissions Due to Crevice Flows in Premixed-Charge Engines," SAE Technical Paper 892085, 1989, doi:10.4271/892085.
39. Alkidas, A. C. "Combustion-chamber crevices: the major source of engine-out hydrocarbon emissions under fully warmed conditions." *Progress in energy and combustion science* 25, No. 3 (1999): 253-273.
40. Mattavi, J., "The Attributes of Fast Burning Rates in Engines," SAE Technical Paper 800920, 1980, doi:10.4271/800920.
41. Poulos, S. and Heywood, J., "The Effect of Chamber Geometry on Spark-Ignition Engine Combustion," SAE Technical Paper 830334, 1983, doi:10.4271/830334.
42. Gamma Technologies GTPower Suite 4 users manual, accessed May 1, 2013.
43. Splitter, D.A., and Szybist, J.P., "Experimental Investigation of Spark-Ignited Combustion with High-Octane Biofuels and EGR. 1. Engine Load Range and Downsize Downspeed Opportunity." Energy & Fuels, 2013, DOI:10.1021/ef401574p.
44. EPA Test Car List Data Files, available at http://www.epa.gov/otaq/tcldata.htm, accessed May 2, 2013.
45. Fraser, N., Blaxill, H., Lumsden, G., and Bassett, M., "Challenges for Increased Efficiency through Gasoline Engine Downsizing," *SAE Int. J. Engines* 2(1):991-1008, 2009, doi:10.4271/2009-01-1053.
46. Bozza, F., Gimelli, A., Strazzullo, L., Torella, E. et al., "Steady-State and Transient Operation Simulation of a "Downsized" Turbocharged SI Engine," SAE Technical Paper 2007-01-0381, 2007, doi:10.4271/2007-01-0381.
47. Keidel, S., Wetzel, P., Biller, B., Bevan, K. et al., "Diesel Engine Fuel Economy Improvement Enabled by Supercharging and Downspeeding," *SAE Int. J. Commer. Veh.* 5(2):483-493, 2012, doi:10.4271/2012-01-1941.
48. Hoyer, K., Sellnau, M., Sinnamon, J., and Husted, H., "Boost System Development for Gasoline Direct-Injection Compression-Ignition (GDCI)," *SAE Int. J. Engines* 6(2):815-826, 2013, doi:10.4271/2013-01-0928.
49. Sellnau, M., Foster, M., Hoyer, K., Moore, W. et al., "Development of a Gasoline Direct Injection Gasoline (GDCI) Engine," *SAE Int. J. Engines* 7():in press, 2014.